Nonlinear dynamical shaping of the fitness landscape of an evolving tumor to combat competitive release

Jeffrey West[a], Yongqian Ma[b], Paul K. Newton[b,c,d,*]

[a]*Integrated Mathematical Oncology Department, H. Lee Moffitt Cancer Center & Research Institute, 12902 Magnolia Drive, SRB 4 Rm 24000H Tampa, Florida, 33612*

[b]*Department of Physics and Astronomy, University of Southern California, Los Angeles, CA, USA*

[c]*Department of Aerospace & Mechanical Engineering, University of Southern California, Los Angeles, CA, 90089-1234 USA*

[d]*Department of Mathematics, Norris Comprehensive Cancer Center, University of Southern California, Los Angeles, CA, USA*

Abstract

The development of chemotherapeutic resistance resulting in tumor relapse is thought largely to be a consequence of the mechanism of *competitive release* of pre-existing resistant cells in the tumor that are selected for growth after chemotherapeutic agents attack the population of chemo-sensitive cells which had previously dominated the collection of competing subclones. To study this process, we use an evolutionary game theory model, with a prisoner's dilemma payoff matrix, based on a system of coupled replicator equations quantifying the clonal competition among three groups of cells: healthy cells (H), sensitive cells (S), and resistant cells (R). Maximum tolerated dose (MTD) schedules are effective at reducing the sensitive cell population which initially shrinks the tumor volume, but releases the resistant cells to re-populate and eventually re-grow the tumor in a more dangerous resistant form. By monitoring the state space associated with the three populations of cells as a coupled nonlinear dynamical system and using the nullcline structure of the system, we show how one can steer the tumor away from the resistant state with an adaptive chemotherapeutic schedule. The control parameters in our model adjust the selection pressure on the various subclones, which effectively allows us to tailor the fitness landscape to suppress the growth of the resistant population while keeping the sensitive population at low enough levels so the tumor volume remains small.

Keywords: competitive release; evolutionary dynamics; adaptive therapy; chemotherapeutic resistance; prisoner's dilemma; replicator dynamics; evolutionary game theory; adaptive control

*corresponding author

Email addresses: runningwest@gmail.com (Jeffrey West), yongqiam@usc.edu (Yongqian Ma), newton@usc.edu (Paul K. Newton)

1. Introduction

In his now classic 1961 study of competition for space between two species of barnacles in the intertidal zone off the Scottish coast, Joseph Connell [1] discovered something interesting. The blue barnacles *Balanus* normally occupied the intertidal zone, while the brown barnacles *Chthamalus* occupied the coast above high tide. Despite the commonly held belief that each occupied their own niche because of different adaptations to local micro-conditions, Connell hypothesized that the colonization of the intertidal zone by *Balanus* was actually preventing *Chthamalus* from inhabiting this region. To test this, he removed the blue barnacles from the intertidal zone and tracked the subsequent penetration of *Chthamalus* into this region. He concluded that *Chthamalus* had undergone *relief from competition* with *Balanus* which allowed it to flourish where previously it could not. The point, he emphasized, was there was nothing *inherent* about the micro-environment of the intertidal zone that was preventing *Chthamalus* from occupying this region. It was simply the competition against a more dominant species that was holding it back. Without the presence of that species, *Chthamalus* happily claimed both zones as fundamental niches. Thus, the important notion of *competitive release* was formulated (see Grant [2]). When two (or more) sub-species compete for the same resources, with one species dominating the other, if the dominant species is removed, this can provide the needed release from competition that can allow the less dominant species to flourish. The mirror image of competitive release is the related notion of *character displacement* developed by Brown and Wilson [3] in which competition can serve to displace one or more morphological, ecological, behavioral, or physiological characteristics of two closely related species that develop in close proximity. These concepts are now well established as part of the overall framework of co-evolutionary ecology theory.

Since co-evolution among competing subclones is now a well established [4, 5, 6, 7] process in malignant tumors, the mechanism of competitive release should be expected to play a role and affect the chemotherapeutic strategies one might choose to eliminate or control tumor growth. Indeed, tumor relapse and the development of chemo-therapeutic resistance is now thought largely to be a consequence of the mechanism of competitive release of pre-existing resistant cells in the tumor which are selected for growth after chemotherapeutic agents attack the subpopulation of chemo-sensitive cells which had previously dominated the collection of competing subclones. Anticancer therapies strongly target sensitive cells in a tumor, selecting for resistance cell types and, if total eradication of all cancer cells is not accomplished, the tumor will recur as derived from resistant cells that survived initial therapy [8]. A schematic of a three compartment model of competitive release is shown in figure 1, where the tumor consisting of sensitive and resistant cells is competing with the surrounding healthy tissue. At diagnosis (see figure 1, left), the tumor is dominated by sensitive cells (red) which out competes the surrounding healthy population (blue) during unhindered tumor progression. A small portion of resistant cells (green) remains in small numbers, suppressed by the larger sensitive population. After several rounds of chemotherapy, the tumor shrinks, leaving the resistant population largely unaffected (figure 1, middle). Inevitably, the tumor relapses due to the small number of cancer cells remaining after therapy (figure 1, right). In the absence of competition from the dominant sensitive population,

the resistant cells grow unhindered, rendering subsequent rounds of chemotherapy less effective. Subsequent application of identical therapies will have a diminished effect. Figure 2 shows the process in a 'Müller fishplot', which we will use later to track the subclonal populations. This representation was first utilized in cancer to compare modes of clonal evolution in acute myeloid leukemia (see [9]). A fishplot shows the tumor burden (vertical axis) over time (horizontal axis) and the clonal lineages (a subclone is encased inside of the founding parent clone in the graph). Figure 2 displays a schematic of unhindered tumor growth after the first driver mutation (figure 2, left). Before diagnosis, the tumor grows exponentially, during which time a resistant mutation occurs (figure 2, middle). After diagnosis, a regimen of continuous chemotherapy shows initial good response and tumor regression, but the resistant population grows back (although at a slower growth rate) unhindered by competition, leading to relapse (figure 2, right). A recent (2012) systematic literature analysis of cancer relapse and therapeutic research showed that while evolutionary terms rarely appeared in papers studying therapeutic relapse since 1980 ($< 1\%$), the language usage has steadily increased more recently, due to a huge potential benefit of studying therapeutic relapse from an evolutionary perspective [10].

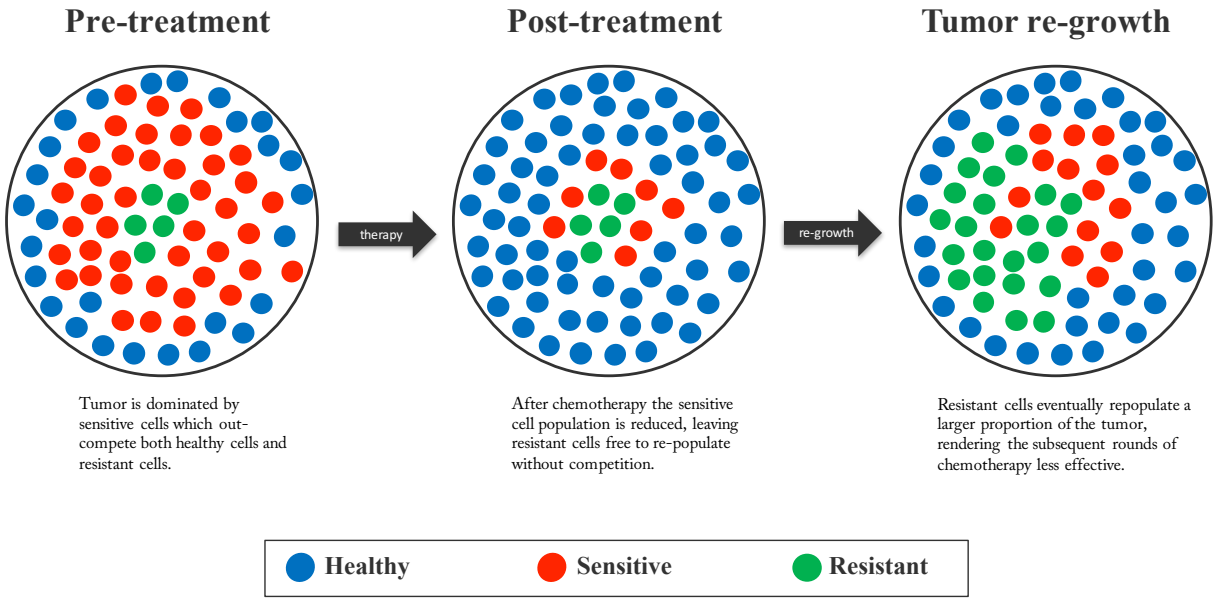

Figure 1: **Schematic of competitive release in a tumor** — (a) Prior to treatment, a tumor consists of a large population of sensitive cells (red) and a small population of less fit resistant cells (green) competing for resources with the surrounding healthy cells (blue); (b) Chemotherapy targets the sensitive population (middle), selecting for the less fit resistant population that thrives in the absence of competition from the sensitive population; (c) Upon regrowth, the tumor composition has larger numbers of resistant cells, rendering the subsequent rounds of treatment less effective.

Our goal in this paper is to describe an evolutionary mathematical model of competitive release in a tumor in order to better quantify and understand the key mechanism responsible

for the evolution of chemo-therapeutic resistance with the hope that understanding it could ultimately prove useful for controlling and harnessing the evolutionary engine that drives its growth. We develop quantitative tools from nonlinear dynamical systems theory which use the current global state of the system with respect to the nullcline curves of the equations to shape the fitness landscape so that the resistant cell population is suppressed while the sensitive cell population stays below a threshold level. The chemotherapeutic strategies that we implement are ones that can adapt on the same timescale as the inherent timescale of evolution of the subclones comprising the tumor, i.e. are as dynamic as the tumor.

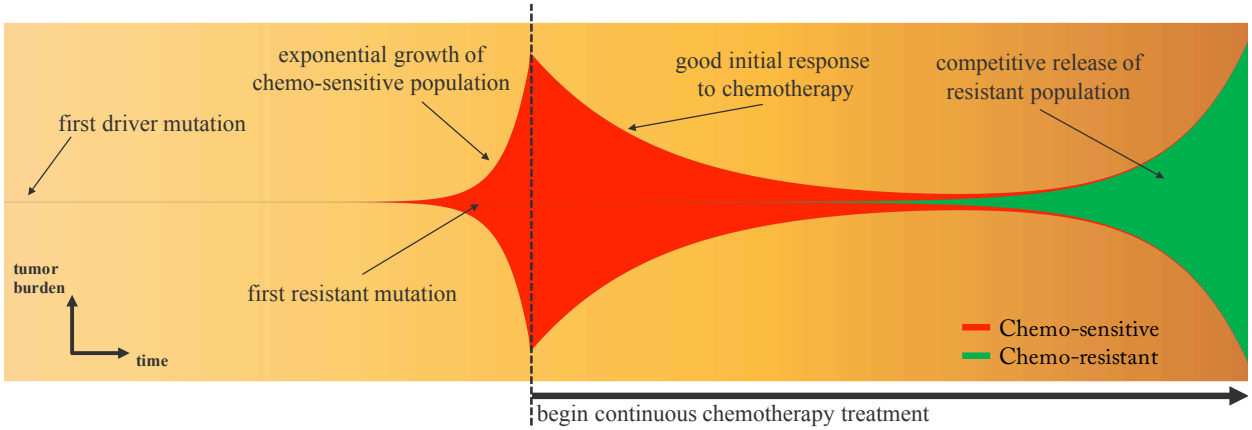

Figure 2: **Clonal evolution of competitive release** — A fishplot (sometimes known as a Müller plot), showing the tumor size (vertical axis) and composition (sensitive: red; resistant: green) over time (horizontal axis, left to right) with important events annotated. After first driver mutation (left), initial exponential growth of sensitive population occurs until diagnosis (dashed line). Continous therapy targeting the chemo-sensitive population responds well with a decrease in tumor burden. In the absence of sensitive cells, the resistant population (existing in small numbers before the start of therapy) grows to become the dominant clone at relapse, albeit typically with lower exponential growth rate.

1.1. Pre-existing resistance

Cancer therapies have shown success in reducing tumor burden for significant time periods, but eventual relapse and resistance have led many to use evolutionary principles and mathematical modeling to address the question of whether resistance arises at some point during therapy or is pre-existing before therapy. It is thought that pre-existing resistant sub-clones should generally be present in all patients with late-stage metastatic disease (for single point mutations which confer resistance), a conclusion supported by probabilistic models [11] and from tumor samples taken prior to treatment [12, 13] which have been reported for melanoma [14], prostate cancer [15], colorectal cancer [16, 17], ovarian cancer [18], and medulloblastoma [19]. According to this view, treatment failure would not be due to *evolution* of resistance during therapy, but rather the pre-existing presence of resistant phenotypes that are relatively sheltered from the toxic effects of therapy [20].

The likelihood of pre-existing resistance has important therapeutic implications. If we assume no pre-existing resistance, then most models predict maximum dose-density therapy

will reduce the probability of resistance largely because this treatment minimizes the number of cell-divisions, thereby minimizing the risk of a mutation leading to acquired resistance [20]. By contrast, in pre-existing resistance scenarios, the maximum dose-density therapy strategy lends itself to competitive release due to the evolutionary nature of tumor progression. Most pre-clinical efforts that aim to maximize the short-term effect of the drug on sensitive cells does not significantly affect the long-term control of cancer [11]. This is because the phenomenon of competitive release can occur via the harsh selective pressure imposed by the tumor microenvironment after cancer therapies diminish the presence of the dominant (i.e. the chemo-sensitive) clone. Additionally, the process of metastasis may allow a resistant subclone in the primary tumor to emerge elsewhere [21].

Pre-existing mutations that are responsible for conferring resistance may be associated with a phenotypic cost, or a reduced fitness, compared to the average fitness of the sensitive cell population. Even factoring in this fitness cost, deleterious mutations are still expected to be present in late-stage metastatic cancers [22]. This cost can come in many ways, such as an increased rate of DNA repair, or an active pumping out of the toxic drug across cell membranes. All of these strategies use up a finite energy supply that would otherwise be available for invasion into non-cancerous tissues or proliferation. Tumors that have not yet undergone treatment may possess resistant cells in small numbers because a fitness disadvantage allows the sensitive population to suppress the growth of the resistant population. The rapid removal of chemo-sensitive cells during therapy releases the resistant population from unwanted competition and thereby permits unopposed proliferation of the resistant cell population.

1.2. Using evolutionary principles to model chemotherapy

It is increasingly understood that eradicating most disseminated cancers may be impossible, undermining the typical goal of cancer treatment of killing as many tumor cells as possible [23]. The underlying assumption of this approach has been that a maximum cell-kill will either lead to a cure or, at worst, maximum life extension. Taking cues from agriculturists who have long abandoned the goal of complete eradication of pests in favor of applying insecticides only when infestation exceeds a threshold in the name of "control" over "cure," there are those who advocate for a shift from the cure paradigm in cancer treatments to a control paradigm [23, 24]. The first step in this paradigm shift is viewing tumor progression from an evolutionary lens. As such, any therapeutic methods should take the following parameters into account: the pre-existing fraction of the resistant population in the tumor before therapy and the relative growth rates (i.e. the fitness cost) of resistant subclones.

With an increasingly detailed picture of evolutionary events in a tumor [25], several treatment strategies have been proposed to exploit or predict the evolutionary trajectory of tumor growth and adaptations [26, 27], such as targeting the trunk driver events (i.e. mutational events that are near the 'trunk' of the phylogenetic tree), that would be present in every tumor cell. Additionally, one could also target parallel evolutionary events, forcing the tumor down a specific evolutionary path, resulting in acquired sensitivity (sequential therapy).

Or, one could design dynamic therapies that maintain a stable population of treatment-sensitive cells [21] to keep the tumor volume small. This is the approach we describe in this manuscript. Some have proposed modelling tumorigenesis as a process by which the homeostasis that characterizes healthy tissue is disrupted, which partly explains how the order of treatments can take advantage of an evolutionary double bind [28, 29, 30], thereby predicting tumor adaptations and exploiting that prediction using fundamental evolutionary principles. Regaining homoeostasis might not mean tumour eradication but instead may represent a new state where the patient lives with cancer as a controllable, yet chronic disease [23]. Treatments can be synergized such that evolving resistance to a single drug will increase susceptibility to a different drug. Others are modeling and planning "evolutionary enlightened" therapies, known as "adaptive therapies" that respond to the tumor's adaptations in order to make future treatment decisions. A theoretical framework for these adaptive therapies first developed by Gatenby [31], leverages the notion that pre-existing resistance is typically present only in small population numbers due to a cost of resistance. This less fit phenotype is suppressed in the Darwinian environment of the *untreated* tumor but treatments that are designed to kill maximum numbers of cells remove the competition for the resistant population and ultimately select for that population during tumor relapse[1]. In contrast, the goal of an adaptive therapy is to maintain a stable tumor burden that permits a significant population of chemo-sensitive cells for the purpose of suppressing the less fit but chemo-resistant populations, consistent with the philosophy that it takes an evolutionary strategy to combat an evolving tumor.

Some of these evolutionary ideas were tested experimentally using mouse models to optimize adaptive strategies designed to maintain a stable, controllable tumor volume [32, 33]. The two-phase adaptive therapy involved an initial high-dose phase to treat the exponential growth of the tumor and a second phase designed for stable tumor control using a variety of strategies (such as decreasing doses or skipping doses when stability is achieved). Findings suggest that adaptive therapies based on evolutionary treatment strategies that maintain a residual population of chemo-sensitive cells may be clinically viable, and is currently extended to an on-going clinical trial (NCT02415621).

With these advances in mind, the goal of this manuscript is to introduce an evolutionary framework to model the important parameters of competitive release and use that framework to better understand therapeutic implications of the tumor evolution. We use a three-component replicator system with a prisoner's dilemma payoff matrix [34] to model the three relevant subclonal populations: healthy cells (H), sensitive cells (S), and resistant cells (R). Using the nullcline information in a triangular phase plane representation of the nonlinear dynamics of the tumor, we first show the essential ingredients that render competitive release possible. Then, using the parameters that control selection pressure (hence relative growth rates) on the three subclonal populations, we attempt to maintain the tumor volume at low levels so that the resistant population does not reach fixation. The upshot of our approach

[1]It is important to note that both high-dose, maximum tolerated dose schedules and low-dose, metronomic dose schedules have this cumulative goal of achieving maximum cell-kill over the course of many cycles of treatment.

could be called 'dynamically shaping the fitness landscape' of the evolving tumor to combat competitive release.

2. Materials and Methods

Previously, a linear combination of exponentials model has been proposed to track the relative tumor volume, $v(t)$, after treatment as a function of the exponential death rate of the sensitive cells, d, the exponential growth rate of the resistant cells, g, and the initial fraction of resistant cells, f [11]. The model can be written as follows:

$$v(t) = (1 - f)e^{-dt} + fe^{gt}. \tag{1}$$

This model, shown to be a reasonably good description of the changing tumor size during therapy for colorectal, prostate, and multiple myeloma cancers, identifies the important parameters in competitive release: initial fractional resistance (f), and birth/death rates (g,d) for the resistant and sensitive populations, respectively. The regrowth rate of the resistant population (g) affects the effectiveness of a continuous therapy (see figure 3a). A greater "cost" of resistance (reflecting by a lower regrowth rate, g) leads to a longer time to relapse. Although the tumor might recur with a slower growth rate, subsequent treatment is ineffective due to resistant population in large numbers. The initial fraction of resistant cells present at the time of treatment, f, also influences treatment effectiveness (figure 3b). An increase in initial fraction leads to a shorter time to relapse. A small difference in resistant regrowth rate (two-fold decrease from $g = 0.2$ to 0.1) leads to an earlier relapse time compared to a large difference in initial fractional resistant (hundred-fold increase from $f = 10^{-6}$ to 10^{-4}), indicating that the regrowth rate parameter has a greater effect on the effectiveness of a continuous therapy (figure 3c). Despite the fact that (1) curve-fits data reasonably well, it contains no evolutionary information or concepts, a keystone principle behind competitive release. Figure 3d - 3f show the results of our evolutionary model (described in the next subsection) with respect to the same effective parameter variations as those from Figure 3a - 3c. The evolutionary model is able to recapitulate the exponential model of equations (1) but has the additional capability of allowing us to track responses to various therapeutic strategies and design new adaptive strategies as the tumor evolves, using a novel technique of shaping the fitness landscape with control parameters to avoid crossing of certain nullclines of the clonal phase space. We describe this technique next.

2.1. The replicator equation model

Our model tracks the evolutionary dynamics of the three competing cell types using the replicator system (see [35]) of equations:

$$\dot{x_i} = (f_i - \langle f \rangle)x_i, \tag{2}$$
$$f_i = 1 - w_i + w_i(A\vec{x})_i. \tag{3}$$

Each of the cells of type i ($i = 1, 2, 3$) competes according to equation (2), where $\vec{x} = (x_1, x_2, x_3)^T$ is the vector of the corresponding frequency of healthy (H), sensitive (S) and

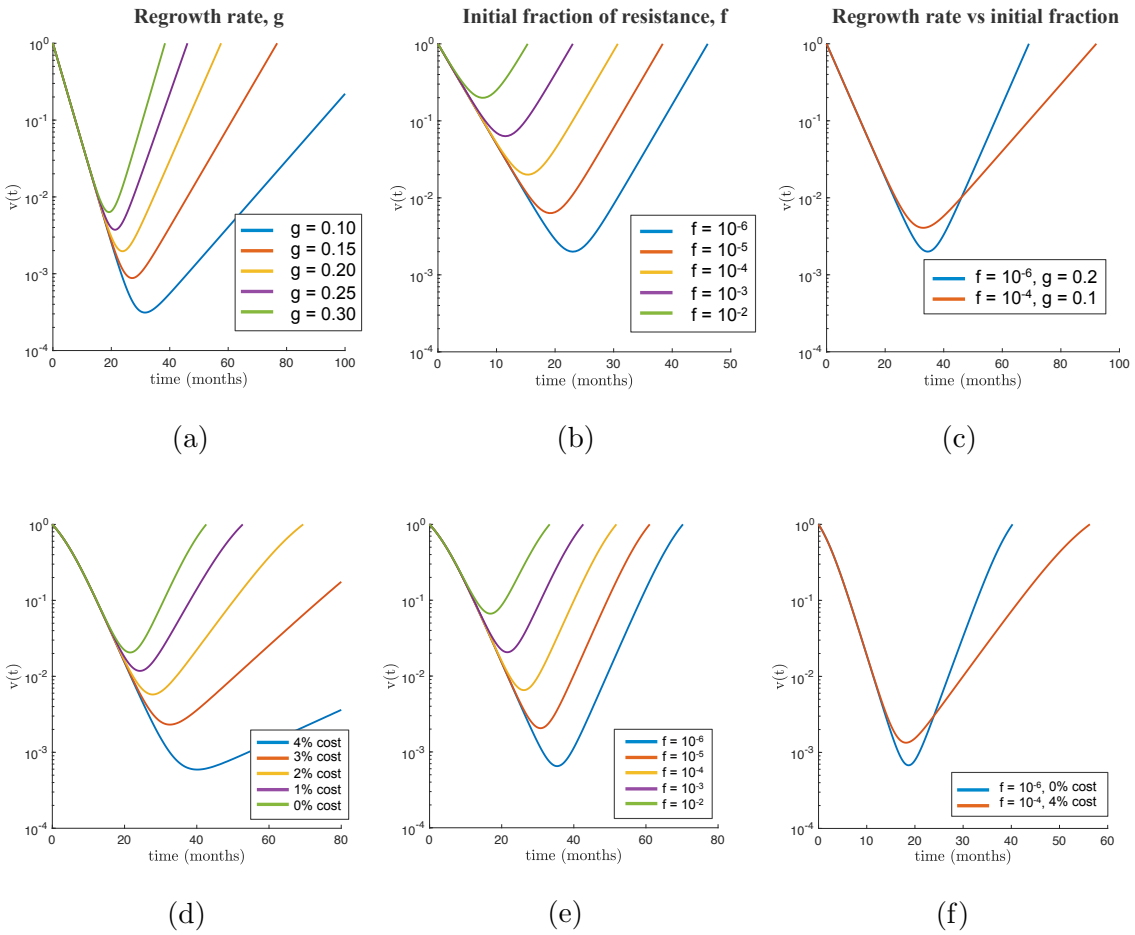

Figure 3: **Dynamics of competitive release under continuous therapy** — The top row (a, b, c) dynamics are described by the simple linear combination of exponential sensitive decay and resistant growth (equation 1). (a) An increase in the resistant regrowth rate ($g = [0.10, 0.15, 0.20, 0.25, 0.30]$) leads to decreased effectiveness of therapy and shorter relapse times ($f = 1e-5; d = 0.3;$). (b) An increased initial fraction of resistance ($f = [1e-6, 1e-5, 1e-4, 1e-3, 1e-2]$) also leads to decreased therapy effectiveness ($g = d = 0.3;$). (c) A small difference in resistant regrowth rate (two-fold decrease from $g = 0.2$ to 0.1) compared to a large difference in initial fractional resistance (hundred-fold increase from $f = 10^{-6}$ to 10^{-4}) shows that the regrowth rate parameter (g) has a greater effect on the effectiveness of a therapy than initial fraction (f). The bottom row (d, e, f) dynamics are described by the evolutionary model (equation 2) and show trends similar to the exponential model. (d) Increasing the phenotypic cost of resistance ($(\alpha - \beta)/\alpha$), results in extended relapse times ($\alpha = 0.02, f = 10^{-3}$). (e) Increased fractional resistance also results in an extended relapse time ($\alpha = \beta = 0.02, f = 10^{-2}$). (f) A low initial fractional resistance ($f = 10^{-6}$) with no cost to resistance (blue) compared with two orders of magnitude greater fractional resistance ($f = 10^{-4}$) with a relatively small cost (cost = 4%) and yet has a shorter time to relapse. This implies that the cost of resistance is more important to relapse than the initial fraction of resistance.

resistant (R) cells, respectively, such that $\sum_i x_i = 1$. The prevalence of each subpopulation, x_i, changes over time according to the changing population fitness, f_i, and the average fitness of all three populations $\langle f \rangle = f_1 x_1 + f_2 x_2 + f_3 x_3$. If the fitness of the subpopulation

is greater than the average fitness, that subpopulation grows exponentially, whereas if it is less, it decays. The fitness is a function of the selection pressure parameters, $w_i; 0 \leq w_i \leq 1$ $(i = 1, 2, 3)$, and the payoff matrix, A. A value of $w_i = 0$ corresponds to neutral drift (no selection) and a value of $w_i = 1$ corresponds to strong selection. $(A\vec{x})_i$ is the ith element of vector $A\vec{x}$.

Before therapy, the selection pressure is constant across all cell types (i.e. $w_i \equiv w$, $i = 1, 2, 3$) at a level that represents the natural selection pressure the tumor environment imposes on the different subpopulations. These values discussed in the literature are typically small, in the range $w_i \equiv w \approx 0.1 - 0.3$. We implement chemotherapy in our model by changing the selection pressure parameters on each of the subpopulations of cells. Values are altered as follows (see figure 4 for explanation of changing fitness landscape):

$$w_1 = (1 + c)w \quad \texttt{(healthy)} \tag{4}$$
$$w_2 = (1 - c)w \quad \texttt{(sensitive)} \tag{5}$$
$$w_3 = w \quad \texttt{(resistant)} \tag{6}$$

Therapy can be administered at different doses (i.e. values of the drug concentration: $c; 0 \leq c \leq 1$). A higher value of c indicates a stronger dose of chemotherapy drug (described in more detail in [36]). This follows the schematic in figure 4 which depicts the change in the fitness landscape before and after therapy.

The fitness landscape (3) is described in detail by the entries of the payoff matrix A, where each pairwise cell-cell interaction is described by the row and column values, which are parameters in the fitness equation (3). The payoff matrix is given by:

$$A = \begin{array}{c} \\ H \\ S \\ R \end{array} \begin{array}{c} \begin{array}{ccc} H & S & R \end{array} \\ \begin{pmatrix} a & b & o \\ h & j & k \\ l & m & n \end{pmatrix} \end{array} \tag{7}$$

There are three pairwise games that can be played, depending on which pairs of cells are interacting at a given timestep: (H, S), (H, R), or (R, S), which are all calculated using a prisoner's dilemma (cooperators, defectors) game, which necessitates the following inequalities: $h > a > j > b$, $l > a > n > o$, and $k > n > j > m$. With this paradigm, the cancer cells act as 'defectors', whereas the healthy cells act as 'cooperators' at each interaction. This scheme has been developed in [34, 37] and discussed at great length, leading to a Gompertzian growth of cancer cells, an increase in the fitness of the cancer population, but an overall decrease in the fitness of the total population of cells. With the two subpopulations of cancer cells in the current model (sensitive and resistant), an interaction between those two treats the sensitive cells as the defectors, with the resistant cells as the cooperators. More discussion of why the prisoners dilemma matrix, which models the evolution of defection, is a useful paradigm for cancer can be found in [34, 37].

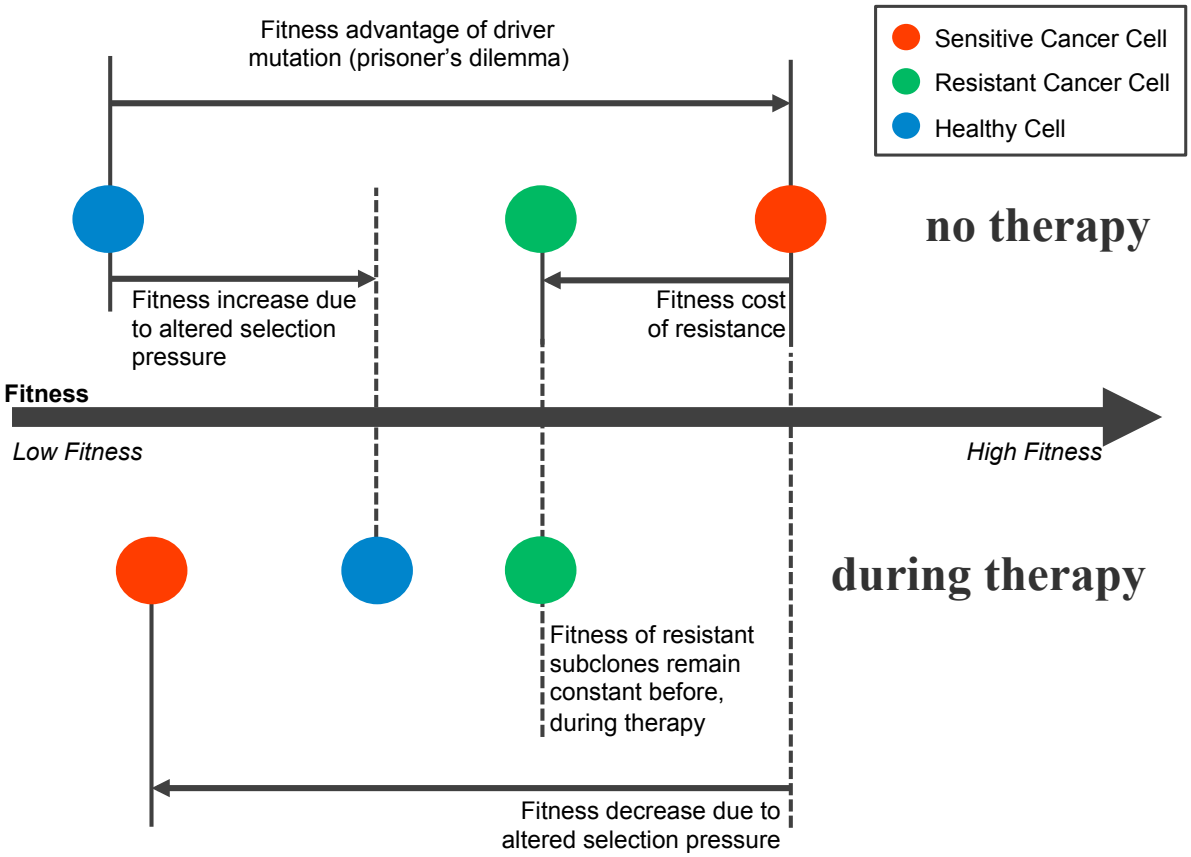

Figure 4: **Fitness landscape before and during therapy** — A schematic of the fitness of each subpopulation before therapy (top) and during therapy (bottom). A driver mutation leads to a fitness advantage of the cancer cell (red), determined by the prisoner's dilemma payoff matrix. A subsequent resistant-conferring mutation comes at a fitness cost (green). The fitness of the resistant population is unaffected by therapy's selective pressure, but the healthy population is given an advantage over the chemo-sensitive population.

2.2. The linearized system and the cost of resistance

The notion of the *cost of resistance* is highlighted in figure 4. With no therapy, the sensitive cells exhibit fastest growth due to their higher fitness value relative to both the resistant population and the healthy population. The difference between the baseline fitness values of the sensitive cells and the resistant cells can be thought of as the 'price paid' by the resistant population to retain their resistance to toxins. This cost, in our model, is quantified as the difference in the (linearized) growth rates of the two populations. Linearizing eqn (2), (3), (which form a cubic nonlinear system if expanded out) gives rise to the sensitive-resistant uncoupled system:

$$\dot{x}_2 = \alpha x_2 \tag{8}$$

$$\dot{x}_3 = \beta x_3, \tag{9}$$

with the growth parameters:

$$\alpha = w_1(1-a) + w_2(h-1) \tag{10}$$
$$\beta = w_1(1-a) + w_3(l-1). \tag{11}$$

Using eqns (4), (5), (6) gives:

$$\alpha = w(h-a) - cw(h+a-2) \tag{12}$$
$$\beta = w(l-a) + cw(1-a). \tag{13}$$

With no therapy, $c = 0$, we have:

$$\alpha = w(h-a) \tag{14}$$
$$\beta = w(l-a). \tag{15}$$

We call the fitness cost of resistance the difference between these growth rates with no therapy, hence $(\alpha - \beta) = w(h-l)$.

3. Results

It is useful to view the nonlinear dynamical trajectories of the system using the trilinear coordinates shown in figure 5a, which gives a representation of the clonal phase space for every possible value of $\vec{x}$. The corners represent saturation of a single cell type (e.g. the top corner represents $\vec{x} = [1, 0, 0]$, or all healthy cells. Figure 5b shows the nullcline information of the dynamical system ($\dot{x}_i = 0$) with therapy off (solid green line) and on (dashed green line). As the trajectory crosses a particular nullcline, the growth ($\dot{x}_i > 0$) / decay ($\dot{x}_i < 0$) on one side switches to decay/growth, allowing for the possibility of trapping an orbit in a closed loop for a finite period of time if the state of the system can be 'steered' appropriately. We do this by altering the dose concentration parameter c in eqns (4) in an off-on (bang-bang) fashion, (5),(6). This is a parameter that can, in principle, be accessed clinically. This is schematically depicted in figure 5b. The dynamics of equation (2) are shown in state space diagrams in Figure 5 for no therapy (figure 5c: $c = 0$) and with therapy (figure 5d: $c = 0.6$). Before treatment, the healthy (H; top corner), sensitive (S; bottom left corner), and resistant (R; bottom right corner) populations compete according to equation (2) and follow trajectories shown (black) in figure 5c. Instantaneous relative velocity is indicated by background color gradient (red to blue). All internal trajectories (pre-therapy) lead to tumor growth and eventual saturation of the sensitive population (bottom left corner). The resistant population nullcline (line of zero growth; $\dot{x}_R = 0$) is plotted in dashed dark red in figure 5c. With no therapy (left), the nullclines divide the triangle into 3 regions. Region 1: $\dot{x}_H > 0$ $\dot{x}_S > 0$ $\dot{x}_R < 0$; Region 2: $\dot{x}_H < 0$ $\dot{x}_S > 0$ $\dot{x}_R < 0$; Region 3: $\dot{x}_H < 0$ $\dot{x}_S > 0$ $\dot{x}_R > 0$. With chemotherapy (right) the selection pressure is altered to the disadvantage of chemo-sensitive cancer population and advantage of the healthy population (shown for $c = 0.6, \alpha = 0.020$, $\beta = 0.018$, $w = 0.1$). In this case the nullclines divide the triangle into 6 regions; Region 1: $\dot{x}_H > 0$ $\dot{x}_S > 0$ $\dot{x}_R < 0$; Region 2: $\dot{x}_H > 0$ $\dot{x}_S < 0$ $\dot{x}_R < 0$; Region 3:

$\dot{x}_H > 0$ $\dot{x}_S < 0$ $\dot{x}_R > 0$;Region 4: $\dot{x}_H < 0$ $\dot{x}_S < 0$ $\dot{x}_R > 0$; Region 5: $\dot{x}_H < 0$ $\dot{x}_S > 0$ $\dot{x}_R > 0$; Region 6: $\dot{x}_H < 0$ $\dot{x}_S > 0$ $\dot{x}_R < 0$. Solution trajectories (black) show the initial trajectory toward healthy saturation (triangle top) but eventual relapse toward resistant population (bottom right of triangle) upon passing the resistant nullcline. The nullclines will be used later to determine timing schedules of adaptive therapy (see figure 7).

3.1. Competitive release in action

Figure 6 details the relationship between dose and two important measures of therapy effectiveness: progression free survival (PFS) and time to relapse. Measuring the effectiveness of a chemotherapy schedule based on the killing rate or progression free survival alone are not sufficient predictive measures of long-term cancer control [11]. As seen in figure 6, left, an increased dose (3 therapies are simulated on identical initial conditions: $\alpha = 0.020$, $\beta = 0.018$, $f = 10^{-3}$) corresponds to a slightly shorter PFS, but an increased time to relapse to the initial tumor volume. However, despite the increase in relapse times, none of these doses optimizes tumor control, as seen in the fishplots (figure 6, right). At the point of relapse to the initial tumor volume, the tumor is dominated by the presence of resistant clones, rendering future treatments ineffective. Oftentimes, the effectiveness of a new chemotherapy drug is be determined by PFS times when drugs that have high killing rates of sensitive cells may have *shorter* times to progression and lower total tumor burden at all times (everything else equal). The figure clearly shows that all treatments have similar progression free times but with a greater range of relapse times (even though continuous treatment always eventually leads to relapse).

The effect of two important parameters of competitive release are shown in 3d - 3f where we vary the cost of resistance (percent cost $= (\alpha - \beta)/\alpha$), and the initial fraction of resistant cells (f). An increased cost of resistance (figure 3d) decreases the regrowth rate and leads to a longer relapse time under continuous therapy. The initial regression rate is identical at the beginning of therapy, but the regrowth rate is diminished by the cost of resistance. An increase in initial fraction of resistance, f, (figure 3e) at the start of therapy leads to shorter relapse times. Although the initial regression rate and the regrowth rate are identical for all simulations (see figure 3e), a small fractional resistance leads to a lower minimum tumor burden achieved and longer relapse times. One can ask which of these parameters has the most significant effect on time to relapse, shown in figure 3f. A low initial fractional resistance with no cost to resistance ($f = 10^{-6}$; 0% cost; shown in blue) is compared to a two orders of magnitude greater fractional resistance ($f = 10^{-4}$) with a relatively small cost ($f = 10^{-2}$; 4% cost; shown in red). Even a small cost (4%) of resistance leads to a significant delay in tumor relapse dynamics, despite a large increase in initial fraction of resistance. This implies that the cost of resistance (i.e. the diminished regrowth rate of the tumor) is more important to relapse than the initial fraction. Note that the results from the evolutionary model (figures 3d - 3f; equation 2) recapitulate the heuristic linear sum of exponentials model (figures 3a - 3c; equation 1) quite well.

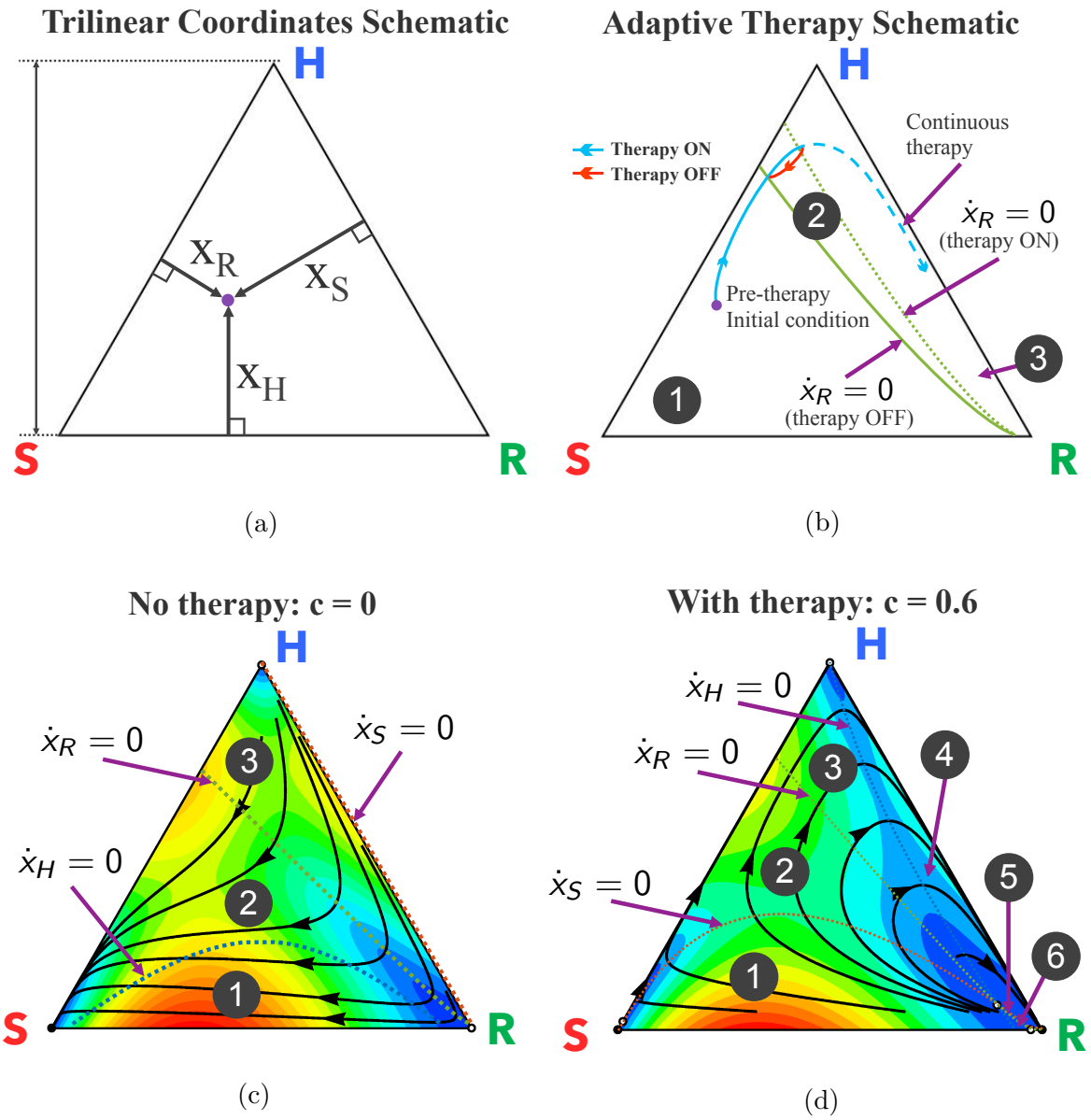

Figure 5: **Dynamic phase portraits before and during chemotherapy** — (a) Trilinear coordinate phase space representation; (b) Schematic of proposed adaptive therapy concept using the resistant nullclines to determine therapy "on" and "off" times in order to trap the tumor in the controllable region 2, and reach approximate cycle that repeats back on itself in red. The continuous therapy is also plotted in dashed blue, for comparison. Two nullclines divide the triangle into 3 regions; region 1: $\dot{x}_R < 0$ for both therapy on and off; region 2:$\dot{x}_R > 0$ for therapy off and $\dot{x}_R < 0$ for therapy on; region 3: $\dot{x}_R > 0$ for both therapy on and off.

Figure 5: (c) Before chemotherapy, the healthy (H), sensitive (S), and resistant (R) populations compete on a dynamical fitness landscape, with several solution trajectories shown (black) and the instantaneous relative velocity indicated by background color gradient (red to blue). All internal trajectories lead to tumor growth and eventual saturation of the sensitive population (bottom left corner). Each population nullcline (line of zero growth: $\dot{x}_i = 0$) is plotted: healthy (dashed blue), sensitive (dashed red), and resistant (dashed green). The nullclines divide the triangle into 3 regions. Region 1: $\dot{x}_H > 0$ $\dot{x}_S > 0$ $\dot{x}_R < 0$; Region 2: $\dot{x}_H < 0$ $\dot{x}_S > 0$ $\dot{x}_R < 0$; Region 3: $\dot{x}_H < 0$ $\dot{x}_S > 0$ $\dot{x}_R > 0$; (d) Chemotherapy alters the selection pressure to the disadvantage of chemo-sensitive cancer population and advantage of the healthy population (shown for $c = 0.6, \alpha = 0.020, \beta = 0.018, w = 0.1$). In this case, the nullclines divide the triangle into 6 regions; Region 1: $\dot{x}_H > 0$ $\dot{x}_S > 0$ $\dot{x}_R < 0$; Region 2: $\dot{x}_H > 0$ $\dot{x}_S < 0$ $\dot{x}_R < 0$; Region 3: $\dot{x}_H > 0$ $\dot{x}_S < 0$ $\dot{x}_R > 0$;Region 4: $\dot{x}_H < 0$ $\dot{x}_S < 0$ $\dot{x}_R > 0$; Region 5: $\dot{x}_H < 0$ $\dot{x}_S > 0$ $\dot{x}_R > 0$; Region 6: $\dot{x}_H < 0$ $\dot{x}_S > 0$ $\dot{x}_R < 0$; Solution trajectories (black) show initial trajectory toward healthy saturation (triangle top) but eventual relapse toward resistant population (bottom right of triangle) upon passing the resistant nullcline.

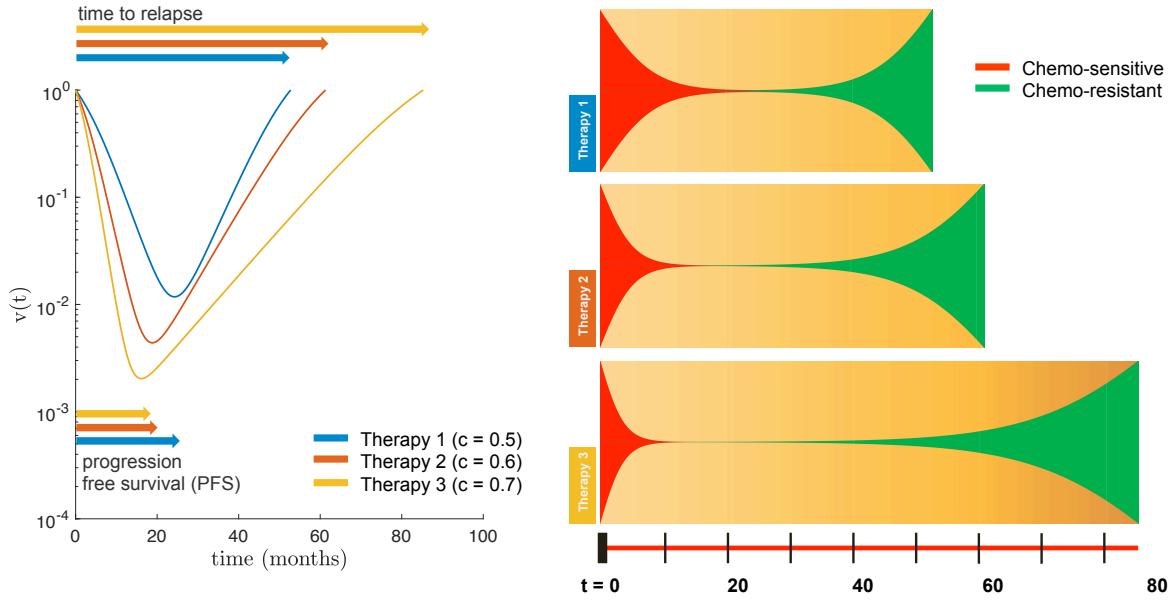

(a) (b)

Figure 6: **The effect of dose on tumor relapse and progression free survival under continuous therapy** — (a) Three therapies are simulated on identical initial conditions ($\alpha = 0.020, \beta = 0.018, f = 10^{-3}, w = 0.1$). Time to relapse significantly increases with increasing dose while the progression free survival shows marginal, but decreasing, difference; (b) The same three therapies are shown in a fish plot, where the simulation is stopped at the point of relapse to initial tumor size (now consisting entirely of chemo-resistant population).

3.2. Managing competitive release

Adaptive therapies take advantage of the important recognition that fitness is contextual and changes during therapy or on drug holidays. The mechanism for control is also contextual. The suppression of the growth of resistant cell population occurs during periods of rest or weaker doses of therapy (drug-sensitive cells have a fitness advantage in these conditions); suppression of the growth of the sensitive cell population occurs during treatment. Figure 7 shows how the idea of contextual fitness can be applied to therapeutic strategies.

A simple control paradigm is proposed to *indirectly* control the resistant population. Therapy targets only the chemo-sensitive cells, but the resistant population can be controlled by systematically choosing when to administer therapy and when to give drug holidays. Therapy "on" is for the purpose of killing sensitive cells. Therapy "off" is for the purpose of allowing a sufficient number of sensitive cells to remain, in order to suppress the resistant population. The control paradigm is as follows: a continuous dose of therapy is administered until the nullcline ($\dot{x}_R = 0$) is reached (see figure 5, right). This is the starting point of positive growth for the resistant population (further therapy would result in $\dot{x}_R > 0$). At this point, a drug holiday (no therapy administered) is imposed until the second nullcline is reached (see figure 5, left). The sensitive population is allowed to regrow until it is large enough to suppress the resistant population once again (and when $\dot{x}_R = 0$). Therapy is administered to allow the tumor to cycle back and forth between the two nullclines. This bang-bang (on-off) strategy allows an extension of relapse times.

This control paradigm is seen in figure 7 for identical initial conditions using a range of drug concentration dose values (low dose: blue; medium dose: red; high dose: yellow). The low and medium dose adaptive therapy strategies adequately outperform the continuous, constant dose (dashed lines). As seen in the fishplots on the right, the resistant population (green) is suppressed during the "off" times of drug holidays, leading to an extended time without relapse. However, a higher dose (during therapy "on") results in diminished tumor control and eventual relapse.

The low- and medium-dose adaptive therapy strategies are successful for two reasons. First, the drug holidays allow an adequate sensitive population size to suppress the growth of the lower-fitness resistant population. Second, the resistant population is never allowed to reach a positive growth ($\dot{x}_R > 0$).

4. Discussion

The chemotherapeutic scheduling strategies outlined in this paper cannot be pre-planned by the oncologist at the beginning of therapy like classical strategies [38], as they rely on significant decision making and continuous monitoring of the different subpopulations of cells that co-evolve as the tumor progresses. This means that the quality of the cell population monitoring system is crucial to the entire strategy, as has been pointed out in [39]. There can be no adaptive tumor control strategy without continuous monitoring of the sub-clones. In addition, the information gleaned from a detailed monitoring system cannot be acted upon unless the various administered drugs are sufficiently targeted to act efficiently and exclusively on specific sub-clones. These two systems must be in place

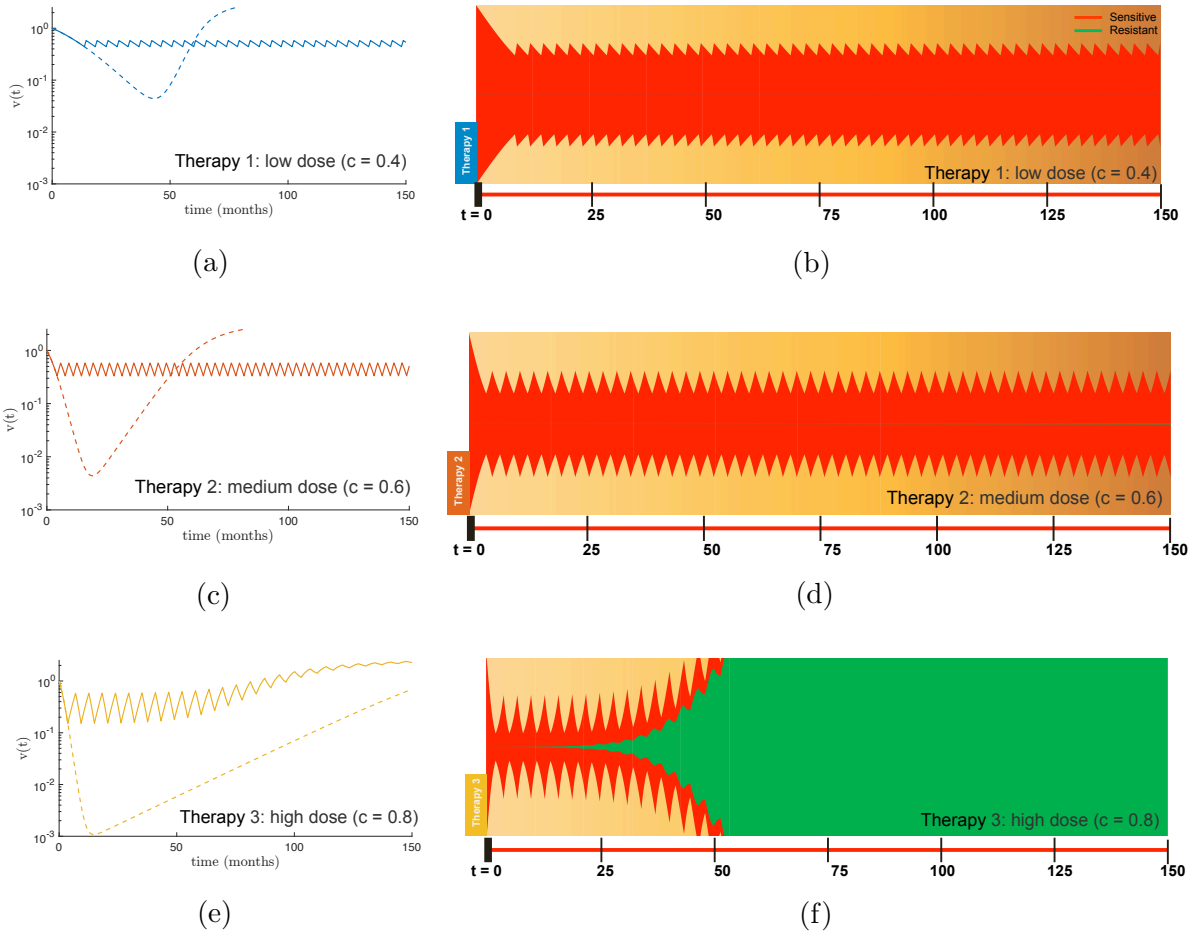

Figure 7: **Adaptive therapy strategy to control resistant population**. In each case, the adaptive therapy control paradigm administers therapy (ON) until the nullcline is reached ($x_R = 0$; see figure 5b). At this point, further therapy will result in the growth of the resistant population (i.e. $x_R > 0$). Therapy is then turned OFF (a drug "holiday") until the second nullcline is reached (see figure 5b), allowing the sensitive population to regain a stable and adequate size useful to suppress the resistant population. This control paradigm works well for low and medium dose, but stable control is not achieved for high dose. (a) Low dose therapy (blue; top: $c = 0.4$) for continuous therapy (dashed line) and adaptive therapy (solid line); (b) Corresponding fishplot; (c) Medium dose therapy (red; middle: $c = 0.6$) for continuous therapy (dashed line) and adaptive therapy (solid line); (d) Corresponding fishplot; (e) High dose therapy (yellow; bottom: $c = 0.8$) for continuous therapy (dashed line) and adaptive therapy (solid line); (f) Corresponding fishplot.

(sensing and actuating) in order to successfully shape the fitness landscape and steer a growth trajectory in a desired direction. We also want to emphasize a separate point, which is that it is not enough to know in detail the *current* state of the system in order to steer it successfully. One must also have a description of all possible *nearby* states of the system, both under therapeutic pressure and without therapy. Better yet is to have a global picture of *all* possible states of the system, with nonlinear nullcline information, as one would obtain by analyzing the full phase space of the entire system. With this information, one would know *where* to steer the system to get to a desired state, even if one does not know *how* to achieve this (clinically). In current state-of-the-art medical practice, such sophisticated sensor-actuator capability is not yet sufficiently developed as it is in many engineering contexts where adaptive control theory is routinely used. Many similar challenges, and the necessary steps towards their implementation, present themselves in the ecology and pest control communities, and we point to Gould's article [40] for a nice early overview. More recently, connections between the approaches developed in the past by ecologists and possible future strategies for oncologists have been discussed by Gatenby and collaborators [41]. Other groups [42, 43, 44] have also developed highly mathematical approaches to tumor control from different points of view. Clearly not all of the clinical steps are in place to effectively test and implement many of the strategies that have been explored theoretically. Yet it is still important to continue to develop the kinds of mathematical models and computer simulations that would serve to identify the many possible schemes, parameter ranges, and sensitivities that could one day be tested via clinical trials that focus on adaptive therapies with the goal of suppression of potential evolution of resistance.

References

[1] J. H. Connell, The influence of interspecific competition and other factors on the distribution of the barnacle chthamalus stellatus, Ecology 42 (4) (1961) 710–723.
[2] P. R. Grant, Convergent and divergent character displacement, Biological journal of the Linnean Society 4 (1) (1972) 39–68.
[3] W. L. Brown, E. O. Wilson, Character displacement, Systematic Zoology 5 (2) (1956) 49–64.
[4] L. M. Merlo, J. W. Pepper, B. J. Reid, C. C. Maley, Cancer as an evolutionary and ecological process, Nature Reviews Cancer 6 (12) (2006) 924–935.
[5] C. S.-O. Attolini, F. Michor, Evolutionary theory of cancer, Annals of the New York Academy of Sciences 1168 (1) (2009) 23–51.
[6] P. C. Nowell, The clonal evolution of tumor cell populations, Science 194 (4260) (1976) 23–28.
[7] M. Greaves, C. C. Maley, Clonal evolution in cancer, Nature 481 (7381) (2012) 306–313.
[8] M. C. Perry, The Chemotherapy Source Book, Lippincott Williams & Wilkins, 2008.
[9] L. Ding, T. J. Ley, D. E. Larson, C. A. Miller, D. C. Koboldt, J. S. Welch, J. K. Ritchey, M. A. Young, T. Lamprecht, M. D. McLellan, et al., Clonal evolution in relapsed acute myeloid leukaemia revealed by whole-genome sequencing, Nature 481 (7382) (2012) 506–510.
[10] C. A. Aktipis, V. S. Kwan, K. A. Johnson, S. L. Neuberg, C. C. Maley, Overlooking evolution: a systematic analysis of cancer relapse and therapeutic resistance research, PloS One 6 (11) (2011) e26100.
[11] I. Bozic, M. A. Nowak, Resisting resistance, Annual Review of Cancer Biology.
[12] K.-A. Kreuzer, P. Le Coutre, O. Landt, I.-K. Na, M. Schwarz, K. Schultheis, A. Hochhaus, B. Dörken, Preexistence and evolution of imatinib mesylate-resistant clones in chronic myelogenous leukemia detected by a pna-based pcr clamping technique, Annals of Hematology 82 (5) (2003) 284–289.

[13] C. Roche-Lestienne, C. Preudhomme, Mutations in the abl kinase domain pre-exist the onset of imatinib treatment, in: Seminars in Hematology, Vol. 40, Elsevier, 2003, pp. 80–82.
[14] K. Kemper, O. Krijgsman, P. Cornelissen-Steijger, A. Shahrabi, F. Weeber, J.-Y. Song, T. Kuilman, D. J. Vis, L. F. Wessels, E. E. Voest, et al., Intra-and inter-tumor heterogeneity in a vemurafenib-resistant melanoma patient and derived xenografts, EMBO Molecular Medicine 7 (9) (2015) 1104–1118.
[15] A. Romanel, D. G. Tandefelt, V. Conteduca, A. Jayaram, N. Casiraghi, D. Wetterskog, S. Salvi, D. Amadori, Z. Zafeiriou, P. Rescigno, et al., Plasma ar and abiraterone-resistant prostate cancer, Science Translational Medicine 7 (312) (2015) 312re10–312re10.
[16] L. A. Diaz Jr, R. T. Williams, J. Wu, I. Kinde, J. R. Hecht, J. Berlin, B. Allen, I. Bozic, J. G. Reiter, M. A. Nowak, et al., The molecular evolution of acquired resistance to targeted egfr blockade in colorectal cancers, Nature 486 (7404) (2012) 537–540.
[17] P. Laurent-Puig, D. Pekin, C. Normand, S. K. Kotsopoulos, P. Nizard, K. Perez-Toralla, R. Rowell, J. Olson, P. Srinivasan, D. Le Corre, et al., Clinical relevance of kras-mutated subclones detected with picodroplet digital pcr in advanced colorectal cancer treated with anti-egfr therapy, Clinical Cancer Research.
[18] R. F. Schwarz, C. K. Ng, S. L. Cooke, S. Newman, J. Temple, A. M. Piskorz, D. Gale, K. Sayal, M. Murtaza, P. J. Baldwin, et al., Spatial and temporal heterogeneity in high-grade serous ovarian cancer: A phylogenetic analysis, PLoS Med 12 (2) (2015) e1001789.
[19] A. S. Morrissy, L. Garzia, D. J. Shih, S. Zuyderduyn, X. Huang, P. Skowron, M. Remke, F. M. Cavalli, V. Ramaswamy, P. E. Lindsay, et al., Divergent clonal selection dominates medulloblastoma at recurrence, Nature 529 (7586) (2016) 351–357.
[20] P. M. Enriquez-Navas, J. W. Wojtkowiak, R. A. Gatenby, Application of evolutionary principles to cancer therapy, Cancer research 75 (22) (2015) 4675–4680.
[21] S. Venkatesan, C. Swanton, Tumor evolutionary principles: How intratumor heterogeneity influences cancer treatment and outcome., in: American Society of Clinical Oncology educational book. American Society of Clinical Oncology. Meeting, Vol. 35, 2016, p. e141.
[22] I. Bozic, M. A. Nowak, Timing and heterogeneity of mutations associated with drug resistance in metastatic cancers, Proceedings of the National Academy of Sciences 111 (45) (2014) 15964–15968.
[23] R. A. Gatenby, A change of strategy in the war on cancer, Nature 459 (7246) (2009) 508–509.
[24] R. Beckman, G. Schemmarm, C. Yeang, Impact of genetic dynamics and single-cell heterogeneity on the development of personalized non-standard medicine strategies for cancer, Proc. Natl. Acad. Sci. 109 (36) (2012) 14586–14591.
[25] M. Jamal-Hanjani, G. Wilson, N. e. a. McGranahan, Tracking the evolution of non-small-cell lung cancer, New England J. of Medicine 376 (2017) 2109–2121.
[26] J. Foo, M. F, Evolution of resistance to anti-cancer therapy during general dosing schedules, J. Theor. Bio. 263 (2) (2010) 179–188.
[27] J. Foo, M. F, Evolution of acquired resistance to anti-cancer therapy, J. Theor. Bio. 355 (2014) 10–20.
[28] D. Basanta, A. Anderson, Homeostasis back and forth: An eco-evolutionary perspective of cancer, bioRxiv (2016) 092023.
[29] D. Basanta, A. R. Anderson, Exploiting ecological principles to better understand cancer progression and treatment, Interface Focus 3 (4) (2013) 20130020.
[30] D. Basanta, R. A. Gatenby, A. R. Anderson, Exploiting evolution to treat drug resistance: combination therapy and the double bind, Molecular pharmaceutics 9 (4) (2012) 914–921.
[31] R. A. Gatenby, A. S. Silva, R. J. Gillies, B. R. Frieden, Adaptive therapy, Cancer Research 69 (11) (2009) 4894–4903.
[32] P. M. Enriquez-Navas, Y. Kam, T. Das, S. Hassan, A. Silva, P. Foroutan, E. Ruiz, G. Martinez, S. Minton, R. J. Gillies, et al., Exploiting evolutionary principles to prolong tumor control in preclinical models of breast cancer, Science Translational Medicine 8 (327) (2016) 327ra24–327ra24.
[33] S. Seton-Rogers, Chemotherapy: Preventing competitive release, Nature Reviews Cancer 16 (4) (2016) 199–199.
[34] J. West, Z. Hasnain, J. Mason, P. Newton, The prisoner's dilemma as a cancer model, Converg. Sci.

Phys. Oncol. 2 (3).

[35] A. Traulsen, J. C. Claussen, C. Hauert, Coevolutionary dynamics: From finite to infinite populations, Physical Review Letters 95 (23) (2005) 238701.

[36] J. West, P. Newton, Chemotherapeutic dose scheduling based on tumor growth rates: the case for low dose metronomic high entropy therapies, USC Preprint.

[37] J. West, Z. Hasnain, P. Macklin, J. Mason, P. Newton, An evolutionary model of tumor cell kinetics and the emergence of molecular heterogeneity and gompertzian growth, SIAM Review 58 (4) (2016) 716–736.

[38] L. Norton, R. Simon, Tumor size, sensitivity to therapy, and design of treatment schedules, Cancer Treatment Reports 61 (7) (1977) 1307.

[39] A. Fisher, I. Vazquez-Garcia, V. Mustonen, The value of monitoring to control evolving populations, Proc. Natl. Acad. Sci. 112 (4) (2015) 1007–1012.

[40] F. Gould, The evolutionary potential of crop pests, American Scientist 79 (1991) 496–507.

[41] R. A. Gatenby, J. Brown, The evolution and ecology of resistance in cancer therapy, Cold Spring Harbor Perspectives in Medicine.

[42] U. Ledzewicz, H. Schattler, Optimal bang-bang controls for a two-compartmental model in cancer therapy, J. Optimization Theory and Appl. 114 (3) (2002) 609–637.

[43] K. Bratton, U. Ledzewicz, H. Schattler, Modeling and control of heterogeneous tumors under chemotherapy, Biomath Comm. 1 (1).

[44] U. Ledzewicz, S. Wang, H. Schattler, N. Andre, M. Heng, E. Pasquier, On drug resistance and metronomic chemotherapy: A mathematical modeling and optimal control approach, Math. Biosciences and Eng. 14 (1) (2017) 217–235.